Proc. of the 9th Intl. Conf. of Asian Society for Precision Engg. and Nanotechnology (ASPEN 2022)
15–18 November 2022, Singapore. Edited by Nai Mui Ling Sharon and A. Senthil Kumar
doi://10.3850/978-981-18-6021-8_OR-17-0085

Effect of β-Ti on surface integrity in slot micro-milling multiphase titanium alloy Ti6Al4V

Yabo Zhang[1,2], Qingshun Bai[1,#], Hao Wang[2,#]

1 School of Mechanical and Electrical Engineering, Harbin Institute of Technology, Harbin 150001, China
2 Department of Mechanical Engineering, Faculty of Engineering, National University of Singapore, 9 Engineering Drive 1, Singapore 117575, Singapore
Corresponding Authors / Emails: qshbai@hit.edu.cn (Q. Bai); mpewhao@nus.edu.sg (H. Wang), TEL: +0451-86402682, FAX: +0451-86402681

KEYWORDS: Surface topography, microstructure evolution, micro-milling, Ti6Al4V

Surface integrity has a significant influence on the fatigue life of micro-components with complex structures. In the present study, surface topography and microstructure evolution of subsurface for the machined surface was investigated by slot micro-milling multiphase titanium alloy Ti6Al4V in terms of chip morphology, burrs formation, surface roughness, surface defects, and subsurface deformation. In particular, the effect of β-Ti was considered in the study. The results show an apparent shear front on the free surface and gouging in the tool-chip contact surface. The up-milling and down-milling present leaf burrs and wave-type burrs with the larger up-milling burr width, respectively. The machined surface shows the obvious feed marks and adhesive materials accompanied by squeezed β-Ti, split β-Ti and plastic side flow β-Ti. The subsurface of the machined surface can be divided into the amorphous layer (24.23 nm), nanocrystalline layer (124.74 nm), and elongated grain layer (197.42 nm), and bulk material due to the coupling effect of thermo-mechanical load. The nanocrystalline layer presents the 10–20 nm dynamic recrystallization grain with a flat shape and distorted elongated subgrains. The elongated grain layer shows the compressed and elongated grains along the slot width direction. The depth of the subsurface deformation layer around β-Ti is 535 nm which is larger than the α-Ti zone. In the deformation layer of machined subsurface. The deformation coordination between α-Ti and β-Ti can lead to the formation of a large number of nanocrystal grains and some enlarged grains in the phase boundary of the α-Ti side. The β-Ti is full of elongated grains and sporadic dynamic recrystallization *nanocrystalline. Our findings contribute to revealing the surface formation mechanism, surface integrity, and fatigue life of micro-milled multiphase parts.*

1 Introduction

Micro-milling is widely used to fabricate some micro components with complex microstructures such as the slow-wave microstructure of terahertz devices [1], micro nozzles in satellites [2], and micro slots of mobile phones [3]. However, it is inevitable to form surface defects and subsurface microstructure evolution in micro-milling, which often lead to stress concentration and microcrack initiation on the machined surface. It can destroy the functional-related performance of micro-components, e.g friction or abrasion contact behaviors, load-bearing capacity, fluid retention properties, and fatigue performance. The subsurface microstructure evolution originates from the plastic deformation of materials and can lead to the mechanical property's variation of material. For polycrystalline or multiphase material such as titanium alloy Ti6Al4V, the microstructure of materials, i. e. grain boundary or phase composition cannot be ignored in micro-milling due to due to the cutting depth close to grain size and phase size. Coordinated deformation between different grains or phases can lead to the uneven surface formation and subsurface microstructure evolution [4]. which may have a negative effect on the micro-components' functional-related performance. To reveal the surface formation mechanism, subsurface deformation mechanism, and improve the functional-related performance of multiphase parts, it is necessary to carry out a depth analysis of the surface formation and subsurface microstructure evolution in slot micro-milling Ti6Al4V.

In this paper, slot micro-milling experiments of Ti6Al4V were carried out to explore the effect of β-Ti on surface integrity. Initially, chip morphology, surface defects, and surface defects were analyzed with the scanning electron microscope (TEM) and high-resolution transmission electron microscopy (HRTEM). Our investigation is of great significance to reveal the surface formation mechanism, surface integrity, and improve the fatigue life of micro-milled multiphase parts. This study enhances the understanding of the surface formation and subsurface formation mechanism in micro-milling Ti6Al4V, which can provide a theoretical basis and practical reference for achieving high surface integrity for polycrystalline or multiphase material by micro-milling

2 Micro-milling experiments set-ups

As shown in Fig. 1, slot micro-milling experiments were conducted on the Kern Evo five-axis ultra-precision micro milling machine. The TiAlN coated micro-milling tool (NS MX235) was adopted in the micro-milling experiments with a diameter of 500 μm and helix angle of 35 degrees. Hot rolling and annealing titanium alloy Ti6Al4V were used in the experiments with the size of 25×5×5 mm. Before the micro-milling, the original surface was trimmed with the milling tool of diameter 3 mm for obtaining a flat surface and ensuring the accurate cutting depth in the micro-milling. The milling parameter is spindle peed 10000 r/min, feed per tooth 0.5 mm/t, and depth of cut 50 µm. After the trimming operation, the machined surface was dry micro-milled with parameters of spindle speed 25000 r/min, feed per tooth 0.7 µm/t, and depth of cut 50 µm.

After micro-milling, surface morphology was observed by SEM, (Phenom Pharos). The surface roughness was obtained by the white light interferometer (Zygo New View 8300). Subsurface images of the machined surfaces were characterized by TEM (200KV, FEI Talos F200X, USA). The TEM samples were prepared with Focused Ion Beam (FIB, FEI Helio). The location of the TEM sample is near the center of the slot at the down-milling side as shown in Fig. 1 (b). The crystallographic information of the atomic scale for the machined surface was discussed by HRTEM. The phase information was identified by the selected area electron diffraction (SAED) patterns.

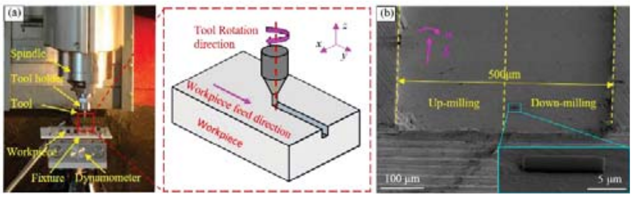

Fig. 1 (a) Experimental equipment and schematic diagram of slot micro milling，(b) SEM images of Ti6Al4V slot and the location of TEM sample

3 Result and Discussion

3.1 Chip morphology and surface morphology in micro-milling Ti6Al4V

The chip morphology of micro-milling Ti6Al4V is shown in Fig. 2. It can be seen from Fig. 2 (a) that the free surface of the chip shows the obvious shear front. The under surface of the chips in Fig. 2 (b) presents the obvious gouging marks. It is reported that the shear front of the chip for multiphase is related to the plastic deformation capacity of the different phases [5]. In micro-milling Ti6Al4V, the softer β-Ti can be extruded out of the free surface to form the ‘quasi shear extrusion chips or shear front in the free surface of the chip.

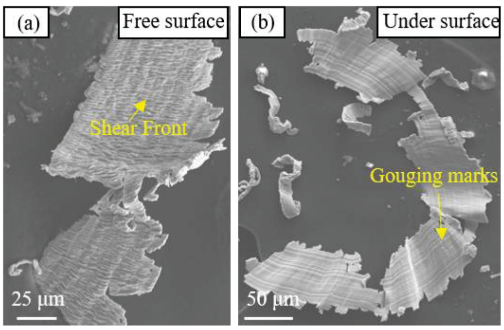

Fig. 2 Chip morphology in micro-milling Ti6Al4V, (a) the free surface, (b) the under surface

Fig. 3 presents the micro slot morphology after micro-milling. It can be seen from Fig. 3 (a) that there is no obvious adhesive chip on the side wall of the up-milling and down-milling sides. The obvious feed marks can be found on the slot bottom, as shown in Fig. 3 (a) and Fig. 3 (b). The surface roughness S_a, S_q, and S_z are 0.078 µm, 0.121 µm, and 3.404 µm, respectively. The slot floor of micro-milling Ti6Al4V has a well-machined surface roughness.

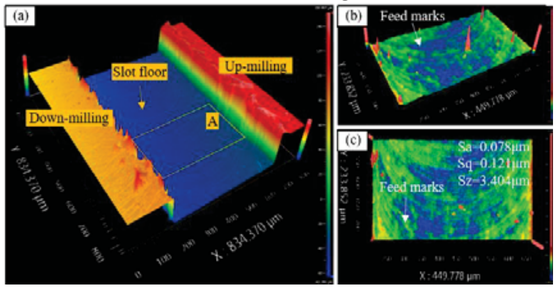

Fig. 3 Three-dimension morphology and surface roughness of the micro-milling Ti6Al4V, (a) micro slot morphology, (b) three-dimension morphology of the slot floor, (c)the surface roughness of the slot floor

The SEM images of the Ti6Al4V slot are presented in Fig. 4. As shown in Fig. 4 (a), there are obvious leaf burrs and wavy type burrs at the up-milling and down-milling, respectively. Moreover, it can be seen from Fig. 4 (b) that there are obvious feed marks and adhesive materials on the slot floor. In Fig. 4, the obvious grain boundary, α-Ti, and β-Ti can be found on the machined surface due to severe contrast differences. To clarify the effect of β-Ti on the surface morphology of the machined surface, Fig. 4 (c) exhibits the enlarged view of the slot bottom. In the titanium alloy Ti6Al4V, α-Ti is the matrix phase. The β-Ti is show the random dots and stripes distribution in the matrix phase as shown in Fig. 4 (c). At the same time, squeezed β-Ti, split β-Ti, and side flow β-Ti can be found on the machined surface due to better plastic deformation of face-centered cubic (FCC) β-Ti than close-packed hexagonal (HCP) α-Ti.

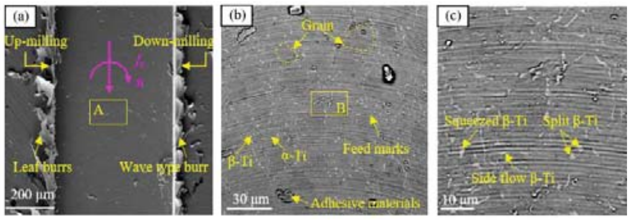

Fig. 4 Burrs and surface defects of the Ti6Al4V slot, (a) the SEM images of the Ti6Al4V slot, (b) the enlarged view of A in (a), (c) the partial enlarged image of (a)

3.2 Subsurface microstructure evolution in micro-milling Ti6Al4V

Fig. 5 shows the diagram of thermal-mechanical distribution for slot floor in slot micro-milling. It is noteworthy that micro-milling is a process of complex thermo-mechanical. The friction between the tool minor flank face and the machined surface can generate a lot of heat on the machined surface. At the same time, the heat can transfer into the workpiece inner along the cutting depth direction due to the temperature gradient difference . The workpiece temperature gradually decays along the cutting depth direction. Moreover, the extrusion and friction between the minor flank face of the micro milling-cutter and the slot floor can lead to composite compressive and shear stresses on the workpiece subsurface. Along the cutting depth direction, the degree of stress concentration and workpiece deformation decreases gradually. The influence depth of heat is smaller than the mechanical layer in micro-milling due to less heat generation between the machined surface and tool flank face, and the fast-cooling process. Therefore, the subsurface of bulk material can be divided into Zone 1 thermal-mechanical effect layer, Zone 2 mechanical effects, and Zone 3 no effect layer, as shown in Fig. 4.

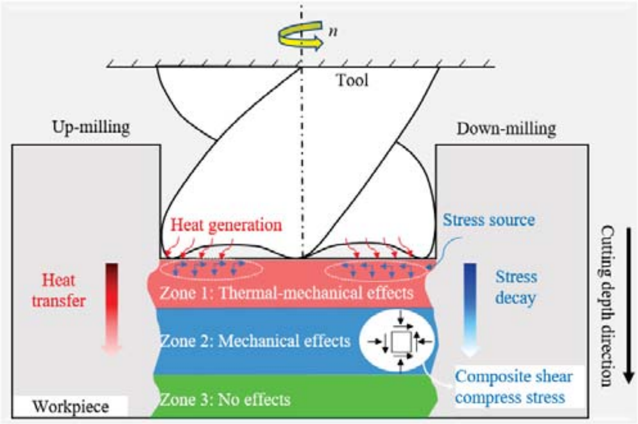

Fig. 5 The schematic diagram of the thermal-mechanical distribution for slot floor in slot micro-milling.

The subsurface bright field (BF) TEM images of the slot floor are present in Fig. 6. With the effect of thermo-mechanical along the cutting depth direction, the subsurface of the slot floor can be divided into the deformed layer with a depth of 346.39 μm and bulk material. According to the microstructure characteristics of the deformed layer and the thermal-mechanical distribution for the slot floor as shown in Fig. 6 and Fig. 5, respectively, the deformed layer can be defined as the 24.23 nm amorphous layer, 124.74 nm nanocrystalline layer, and 197.42 nm elongated grain layer. The nanocrystalline layer is mainly composed of the 30~50 nm nanocrystalline grains and distorted subgrains. Moreover, the shape of nanocrystalline grain is platy, which is different from the traditional circular equiaxed crystal after heat treatment and annealing. In the micro-milling, the obvious extrusion effect between the tool flank face and the slot floor can lead to composite compressive shear stress on the nanocrystalline grains, as shown in Fig. 5, which can lead to the formation of platy nanocrystalline grains. Therefore, dynamic recrystallization occurs in the subsurface of the slot bottom of micro-milling Ti6Al4V. Besides, the composite compressive shear stress on the subsurface of the slot floor can also lead to grain distortion and the formation of compressed elongated grain at 33.8 degrees from horizontal in the enlarged grain layer as shown in Fig. 6.

Fig. 7 presents the Energy-dispersive X-ray spectroscopy (EDS) mapping around the β-Ti on the subsurface of the slot floor. More element vanadium (V) and little element aluminum (Al) in area B illustrate that this area is β-Ti due to vanadium is the stable element of β-Ti. Moreover, the β-Ti of zone B has a large size with a length of around 2 μm and a width of around 500 nm, which indicates that the β-Ti comes from the original workpiece rather than the formation of diffusion phase transformation in the thermal-mechanical load of micro-milling. Moreover, no other enriched element vanadium (V) zone can be found in the selected area in Fig. 7, which illustrates that there is no obvious diffusion phase transformation around the β-Ti on the subsurface of the slot floor.

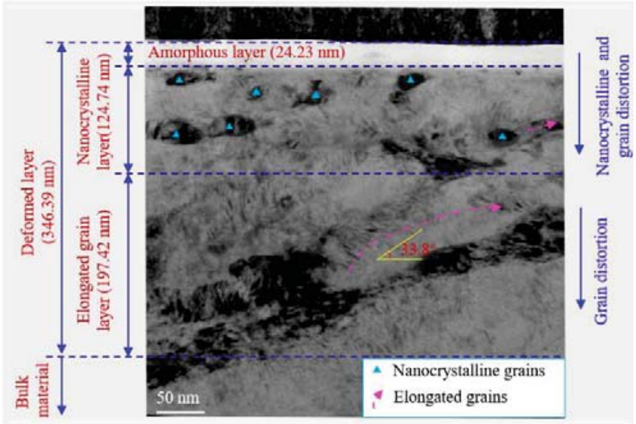

Fig. 6 TEM image of Ti6Al4V slot showing subsurface the microstructure evolution

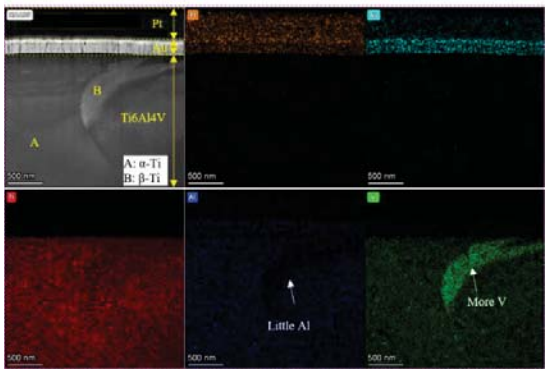

Fig. 7 EDS mapping of the slot subsurface around the β-Ti

The BF and High-angle annular dark-field (HAADF) images in Fig. 8 show the subsurface plastic deformation morphology around the β-Ti of the slot floor. The deformation layer thickness is 535 nm at the β-Ti deformation zone in Fig. 8 (a), which is larger than the α-Ti deformation zone as shown in Fig. 6. At the same time, there are a large number of nanocrystal grains in the phase boundary at the α-Ti side as shown in the green arrow of Fig. 8 (c) and (d). Moreover, Fig. 8 (c) and (d) also show some elongated grains in the phase boundary of the α-Ti side as shown in the red arrows A, B, C, and H. As for the β-Ti, there are some dynamic recrystallization grains and elongated grains in the area close to the workpiece surface, as shown in the yellow arrow and red arrows D, E, F, G, respectively, in Fig. 8 (c), (d), (e) and (f).

In the titanium alloy Ti6Al4V, the crystal structure of α-Ti and β-Ti is close-packed hexagonal (HCP) and face-centered cubic (FCC), respectively. HCP α-Ti has only three independent slip systems and BCC β-Ti has twelve independent slip systems, which make β-Ti have better plastic deformation than α-Ti. At the same time, the plastic deformation mode of the α+β duplex titanium alloy is different from the single-phase α-Ti or β-Ti. There is coordinated deformation between α-Ti and β-Ti. Liu et al [6] investigated the coordinated deformation of the different phases for titanium alloy Ti6Al4V under severe plastic deformation. It is reported that coordinated deformation depends on the relative grain sizes between α-Ti and β-Ti. When the grain size of β-Ti is much smaller than the α-Ti. The plastic deformation firstly occurs in the α-Ti. There is a high-density dislocation structure at the phase interface of the α-Ti side, which can lead to the stress concentration on the phase interface. To coordinate the deformation of α-Ti and β-Ti, the dislocation multiplication of β-Ti occurs on the zone or near zone of the phase interface with the high dislocation density at the side of α-Ti. Then, the dislocation movement can form the dislocation tangle and dislocation wall on the β-Ti side. When the minor axis size of α-Ti is refined to be comparable to the grain size of β-Ti, there are a large number of dislocation slips in β-Ti, which can lead to the dislocation annihilation, dislocation rearrangement, and the formation of subgrains in the β-Ti. With the development of deformation, equiaxed grain or dynamic recrystallization grain can form in the β-Ti. In the slot micro-milling Ti6Al4V, the α-Ti is larger than the β-Ti. The plastic deformation of the workpiece first occurs on the α-Ti side and a large number of nanocrystalline particles of dynamic recrystallization can be found on the phase interface of the α-Ti side. To coordinate the deformation between α-Ti and β-Ti，a large number of elongated deformation grains can be found on β-Ti. Besides, more deep deformed layer depth can be found on the β-titanium.

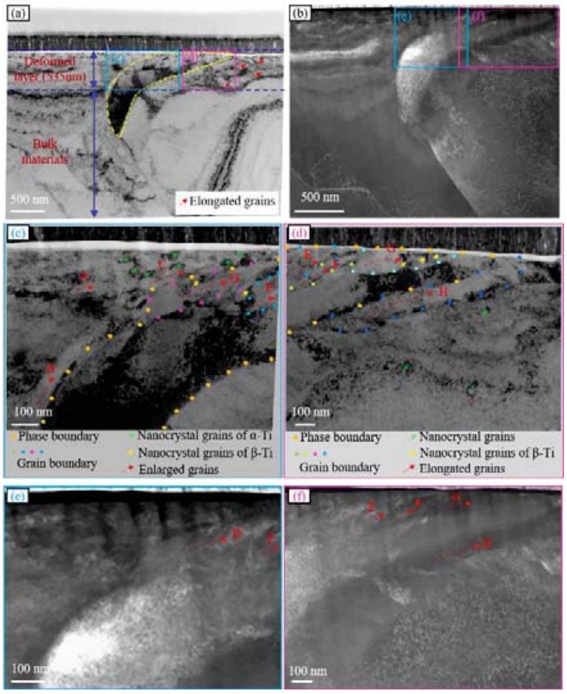

Fig. 8 TEM and HAADF of the subsurface for the slot bottom around the β-Ti, (a) BF-TEM of the β-Ti, (b) HADDF-TEM of β-Ti, (c) partial enlarged image of (a), (e) (f) enlarge HADDF-TEM of (b)

4 Conclusions

In summary, the surface integrity of slot micro-milling Ti6Al4V was investigated by chip formation analysis, surface defects observation, and subsurface microstructure evolution discussion. The main conclusions are as follows:

(1) The chips show the obvious shear front on the free surface due to the extruded β-Ti and gouging marks on the under surface. Leaf burrs and wave-type burrs can be found on the up-milling side and down-milling side, respectively. The surface defects are mainly fed marks, adhesive materials, squeezed β-Ti, split β-Ti, and plastic side flows β-Ti.

(2) The subsurface deformation layer is composed of the amorph ous layer (24.23 nm), the nanocrystalline layer (124.74 nm), the elongated grain layer (197.42 nm), and bulk material with the ef fect of thermo-mechanical load. The 30~50 nm dynamic recrystal lization nanocrystalline with the platy shape and distorted elonga ted grains are full of the nanocrystalline layer. The elongated gr ain layer presents the compressed and elongated grains along th e slot width direction.

(3) The effect of β-Ti can lead to a larger subsurface deformatio n layer thickness (535 nm) than the α-Ti area. A large number of nanocrystal grains and some enlarged grains can be found in the phase boundary of the α-Ti side due to the deformation coo rdination between α-Ti and β-Ti. Elongated grains and sporadic dynamic recrystallization nanocrystalline are presented in β-Ti.

ACKNOWLEDGEMENT

This research work was supported by the National Natural Science Foundation of China (Grant No. 52075129). The authors are also grateful for the financial support of the China Scholarship Council (202006120178). The author is grateful to Mr. Liu Huan, Mr. Li Donghai, and Mr. Xu long for their help in Transmission electron microscope observation and data analysis.

REFERENCES

1. X Wu., L Li., N He., “Investigation on the burr formation mechanism in micro cutting,” Precis. Eng., Vol. 47, pp. 191-196, 2017.
2. Y Cai., Z Liu., Q Song., Z Shi., Y Wan., “Fluid mechanics of internal flow with friction and cutting strategies for micronozzles,” Int. J. Mech. Sci., Vol. 100, pp. 41-49, 2015.
3. D Masato., M Sorgato., P Parenti., M Annoni., G Lucchetta., “Impact of deep cores surface topography generated by micro milling on the demolding force in micro injection molding,” J. Mater. Process. Technol., Vol. 246, pp. 211-223, 2017.
4. Z Wang., J Zhang., J Zhang., G Li., H Zhang., H ul Hassan., A Hartmaier., Y Yan., T Sun., “Towards an understanding of grain boundary step in diamond cutting of polycrystalline copper,” J. Mater. Process. Technol. Vol. 246, pp. 116400, 2020.
5. A Simoneau. , E Ng., M A Elbestawi., “Chip formation during microscale cutting of a medium carbon steel,” Int. J. Mach. Tools Manuf., Vol. 46, No. 5 pp. 467-481, 2006.
6. Y G Liu. , M Q Li., “Structure response characteristics and surface nanocrystallization mechanism of alpha phase in Ti-6Al-4V subjected to high energy shot peening,” J. Alloys Compd., Vol. 773, pp. 860-871, 2019.